Quarksonic matter at high isospin density*

Gaoqing Cao(曹高清)[1] Lianyi He(何联毅)[2] Xu-Guang Huang(黄旭光)[1]

[1] Physics Department and Center for Particle Physics and Field Theory, Fudan University, Shanghai 200433, China
[2] Department of Physics, Tsinghua University and Collaborative Innovation Center of Quantum Matter, Beijing 100084, China

Abstract: Analogous to the quarkyonic matter at high baryon density in which the quark Fermi seas and the baryonic excitations coexist, it is argued that a "quarksonic matter" phase appears at high isospin density where the quark (antiquark) Fermi seas and the mesonic excitations coexist. We explore this phase in detail in both large N_c and asymptotically free limits. In the large N_c limit, we sketch a phase diagram for the quarksonic matter. In the asymptotically free limit, we study the pion superfluidity and thermodynamics of the quarksonic matter by using both perturbative calculations and an effective model.

Keywords: quarksonic matter, isospin density, large N_c, perturbative calculation

PACS: 12.38.Aw, 12.39.Fe, 11.30.Rd **DOI:** 10.1088/1674-1137/41/5/051001

1 Introduction

In 1932, by direct analogy with ordinary spin, Heisenberg introduced the concept of isospin to describe the symmetry between protons and neutrons under the strong interaction [1]. Then, after the discovery of the substructure of hadrons [2], the idea of isospin was naturally transferred to denote the two lightest flavors of quarks, the u and d quarks. Now, isospin is a widely used concept in nuclear and particle physics. Systems with nonzero isospin densities span a large range of nuclear media, from normal nuclei near drip lines to neutron stars [3]. Novel phenomena can happen at high isospin density. For example, it is well known that pion superfluidity can occur at large isospin chemical potential $\mu_{\rm I}$ (or density) [4–12], and such superfluidity experiences a smooth crossover from the Bose-Einstein condensation of pions to Bardeen-Cooper-Schrieffer quark-antiquark pairing (BEC-BCS crossover) with increasing $\mu_{\rm I}$. Moreover, as there is no sign problem at finite $\mu_{\rm I}$, these results have also been studied and verified by lattice quantum chromodynamics (LQCD) simulations [13–15].

Based on large N_c analysis, McLerran and Pisarski argued that, at large baryon chemical potential $\mu_{\rm B}$, a new phase of dense matter can emerge in which the chiral symmetry is restored while the system remains confined at low temperature [16]. They call such a new phase of matter the "quarkyonic matter", reflecting the coexistence of quarks and baryons: the thermodynamic properties of the system are dominated by quark Fermi seas but the elementary fermionic excitations are confined baryons near the Fermi surfaces. Interestingly, recent LQCD simulations showed that even at $N_c = 2$, the notion of quarkyonic matter is serviceable [17]. In this case, LQCD found that deconfinement never happens at zero temperature when $\mu_{\rm B}$ increases; instead, the system at large $\mu_{\rm B}$ is characterized by quarks always residing in Fermi seas and diquark condensate near the Fermi surface.

It is well known that the phase structure of two-color QCD ($\rm QC_2D$) at finite baryon chemical potential $\mu_{\rm B}$ is very similar to that of real QCD at finite isospin chemical potential $\mu_{\rm I}$ [8, 18]. In fact, they are identical in the large N_c limit [19]. Thus, one can anticipate that QCD matter at large isospin density is also quarkyonic matter-like but with a Fermi sea comprising quark (antiquark) isospin charge and elementary excitation near the Fermi surface, the mixing pions, in which some isospin component condenses at low temperature and leads to superfluidity. To be more specific, we call this phase of matter "quarksonic matter". Its physical picture is illustrated in Fig. 1 where the case $\mu_{\rm I} < 0$ is considered. Near the Fermi surface of isospin charge, $\bar{\rm u}$ antiquarks and d quarks pair with each other to form a pion condensate $\langle \pi^- \rangle$ at low temperature. For large enough $|\mu_{\rm I}|$, the pressure and $|\mu_{\rm I}|$ related quantities such as isospin density and compressibility can well be described by nearly free fermion gases of $\bar{\rm u}$ antiquarks and d quarks; but the thermally excited quantities such as entropy and heat capacity can be well described by Goldstone excitation

Received 17 January 2017

∗ Supported by Thousand Young Talents Program of China, Shanghai Natural Science Foundation, (14ZR1403000) and NSFC (11535012), China Postdoctoral Science Foundation (KLH1512072)

Π^+ at low temperature [4, 5]. As temperature increases, the deconfinement phase transition happens at a certain critical temperature $T_{\rm d}$, above which gluons and then quarks (antiquarks) become active thermal excitations.

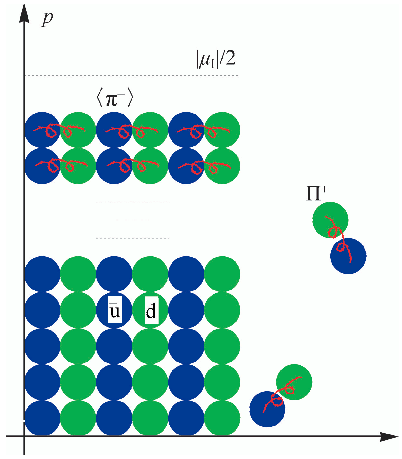

Fig. 1. (color online) The particle distributions in quarksonic matter at low temperature and large isospin density, where the highest dotted line is the Fermi surface $p_{\rm F} = |\mu_{\rm I}|/2$ associated with isospin density, $\langle\pi^-\rangle$ denotes the pion condensate near the Fermi surface and Π^+ denotes the Goldstone boson related to I_3 flavor symmetry breaking. The red spirals represent gluons.

In this work, we will revisit quarksonic matter and its properties in both large $N_{\rm c}$ and asymptotically free limits. In the large $N_{\rm c}$ limit, we will map out a phase diagram in the temperature and isospin chemical potential plane, along with discussions similar to those of quarkyonic matter in Ref. [16]. Some comments on the real QCD phase diagram will be given after that. In the asymptotically free limit, we will first derive the coefficient b_π (see below for the definition) involved in the expression of the pion condensate up to sub-leading order in QCD coupling constant, following Refs. [20, 21], and then perform further numerical calculations by utilizing the effective pure gluodynamics formalism developed in Ref. [11] to study the characteristics of the new quarksonic matter phase.

2 Large $N_{\rm c}$ limit and phase diagram

A real QCD system with $N_{\rm c} = 3$ is strongly coupled at low energy and thus is very difficult to handle. But if one treats $N_{\rm c}$ as a free parameter and lets it go to infinity while keeps $\lambda = g^2 N_{\rm c}$ fixed (the 't Hooft limit) [22], one can greatly simplify the problem and obtain important insights into the original problem. So we will first consider the phase diagram in the $T - |\mu_{\rm I}|$ plane at the large $N_{\rm c}$ limit, which is illustrated in Fig. 2. Two important points should be emphasized. First, as chiral symmetry restoration is usually consistent with the deconfinement transition, only the BCS state is expected to exist above the deconfinement temperature $T_{\rm d}$. Second, due to volume independence in large-$N_{\rm c}$ QCD-like gauge theories [23], all the transition lines below $T_{\rm d}$ are temperature independent, as was pointed out in Ref. [24].

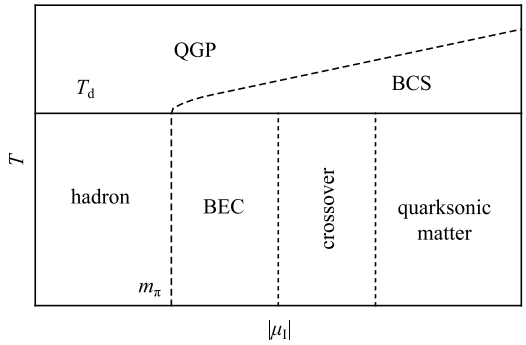

Fig. 2. The $T - |\mu_{\rm I}|$ phase diagram in the large $N_{\rm c}$ limit. The solid, dashed and dotted lines correspond to the first-order transition, second-order transition, and crossover, respectively.

At the large $N_{\rm c}$ limit, the quark loops ($\sim N_{\rm c}^1$) are strongly suppressed compared to gluon loops ($\sim N_{\rm c}^2$) [22], which is responsible for the confining dynamics. As a result, the deconfinement temperature is independent of $|\mu_{\rm I}|$, $T_{\rm d} \sim \Lambda_{\rm QCD}$, where $\Lambda_{\rm QCD}$ is the QCD confinement scale, which is assumed to be $\sim N_{\rm c}^0$. At zero temperature, pion superfluidity happens when $|\mu_{\rm I}|$ is larger than the pion mass in vacuum m_π [4, 5], which is $\sim N_{\rm c}^0$; thus the critical isospin chemical potential is $|\mu_{\rm I}^c| \sim N_{\rm c}^0$. Right above $|\mu_{\rm I}^c|$, the system is a dilute Bose gas of pions and the superfluidity is due to the BEC of the pions. In this region, the pressure is of order $\sim N_{\rm c}^0$, as in the hadronic phase, because almost all the isospin density ($\sim N_{\rm c}^1$) contributes to the BEC, which does not affect the thermodynamic properties. With increasing $\mu_{\rm I}$, the system begins to transform from a BEC of pions to BCS superfluidity of quarks and antiquarks. No symmetry breaking occurs during such a BEC-BCS crossover and thus there is no critical $|\mu_{\rm I}|$ to set this crossover. We mark the starting point of the BEC-BCS crossover as the $|\mu_{\rm I}|$ at which the in-medium quark mass drops to zero $m_{\rm q}(|\mu_{\rm I}|) - |\mu_{\rm I}|/2 = 0$. A $|\mu_{\rm I}|$ determined in this way is also independent of $N_{\rm c}$. Eventually, when $|\mu_{\rm I}|$ is large enough, the pressure is dominated by quark (antiquark) Fermi seas and is of order $\sim N_{\rm c}^1$. We then enter the quarksonic matter phase. Because the interactions among pions are suppressed at the large $N_{\rm c}$ limit, we expect the threshold $|\mu_{\rm I}|$ for this phase to also be $\sim N_{\rm c}^0$. The pion condensate or the quark-antiquark condensate in general increases with $|\mu_{\rm I}|$ and so does the critical temperature T_π for pion superfluidity. Thus, for large enough $|\mu_{\rm I}|$, T_π will eventually be larger than $T_{\rm d}$, leaving the region in between occupied

by deconfined pion superfluid. Above T_π, the system is a quark-gluon plasma (QGP) with pressure $\sim N_c^2$.

For real QCD, the topological structure of the $T-|\mu_I|$ phase diagram is expected to be similar to the one in the large N_c limit. However, some detailed structure may be different. Combining the results from perturbative discussions [4, 5], LQCD calculations [13, 14], and model studies [6, 8], one expects T_d to decrease with increasing $|\mu_I|$ over the whole region (as the confinement scale decreases at large $|\mu_I|$), which indicates shrinking of the quarksonic matter region. The melting temperature of the pion superfluidity keeps increasing with $|\mu_I|$ and the transition is still second order, but it is argues that the deconfinement transition changes from crossover to first order with a new critical end point in the BEC-BCS crossover region [4, 5, 14].

3 Asymptotically free limit

Thanks to the asymptotic freedom of QCD, we can perform perturbative calculations when $|\mu_I|$ is very large. Previously, similar calculations have already been done in the large μ_B limit [20, 21, 25–27], and the expressions of the diquark condensate and the critical temperature of color superconductivity were obtained up to sub-leading order in the perturbative coupling expansion [21, 25]. The expression of the pion condensate (more precisely, the excitation gap of the quasiparticles) was argued to be in the form $\Delta = b_\pi|\mu_I||g|^{-5}e^{-3\pi^2/(2g)}$ with $b_\pi \approx 10^4$ [4, 5]. The actual value of b_π is still unknown so far, so we would like to calculate b_π first within the perturbative framework.

3.1 The coefficient b_π

To obtain the correct value of b_π, we need to self-consistently take the self-energy of quarks into account [21]. Considering pion condensate $\pi^-(\mathrm{K}) \neq 0$, which interacts with quarks through $\bar\psi i\gamma_5\tau^-\pi^-(\mathrm{K})\psi$ where $\tau^\pm = (\tau_1 \pm i\tau_2)/2$, the inverse quark propagator in flavor and energy-momentum spaces is given as

$$G^{-1}(K)=\begin{pmatrix} \not{K}+\mu\gamma_0+\Sigma_{uu}(K) & -i\gamma_5\pi^+(K) \\ -i\gamma_5\pi^-(K) & \not{K}-\mu\gamma_0+\Sigma_{dd}(K)\end{pmatrix}, \quad (1)$$

where we have used $\mu \equiv \mu_I/2$ to simplify the notation and set $\mu_I < 0$. Then the quark propagator can be derived with the elements in flavor space given by

$$\begin{aligned} G_{uu/dd}(K) &= \left([G^0_{uu/dd}(K)]^{-1}+\gamma_5\pi^\pm[G^0_{dd/uu}]^{-1}\gamma_5\pi^\mp\right)^{-1}, \\ G_{ud/du}(K) &= iG^0_{uu/dd}(K)\gamma_5\pi^\pm(K)G_{dd/uu}(K), \end{aligned} \quad (2)$$

where we have defined the free quark propagators with self-energy as

$$G^0_{uu/dd}(K) \equiv [\not{K} \pm \mu\gamma_0 + \Sigma_{uu/dd}(K)]^{-1}. \quad (3)$$

The self-energy can be evaluated to leading order as [21, 28]

$$\Sigma_{uu/dd}(K) = \gamma_0\bar g^2\left(k_0\ln\frac{M^2}{k_0^2}+i\pi|k_0|\right), \quad (4)$$

where $\bar g = g/(3\sqrt{2}\pi)$ and $M^2 = (3\pi/4)m_g^2$ with the gluon mass $m_g^2 = g^2\mu^2/(3\pi^2)$. Because the imaginary parts are suppressed by g compared to the real parts and can be neglected [21], the free quark propagators can be rewritten as

$$G^0_{uu/dd}(K) = [\gamma_0\tilde k_0 - \gamma\cdot\boldsymbol{k} \pm \mu\gamma_0]^{-1}, \quad (5)$$

where $\tilde k_0 = k_0/Z(k_0)$ and $Z(k_0) \equiv [1+\bar g^2\ln(M^2/k_0^2)]^{-1}$.

The gap equations for $\pi^\pm(K)$ can be evaluated in the mean field approximation as

$$i\gamma_5\pi^\pm(K) = g^2\frac{T}{V}\sum_Q \Delta^{ab}_{\mu\nu}(K-Q)\gamma^\mu\lambda_a G_{ud/du}(Q)\gamma^\nu\lambda_b. \quad (6)$$

We will focus on the gap equation for $\pi^-(K)$; the case for $\pi^+(K)$ is similar. The color indices can be easily summed to give the quadratic Casimir operator $C_2(N_c) = 4/3$, and the matrix $-i\gamma_5$ can be cancelled from both sides:

$$\pi^-(K)=\frac{4g^2}{3}\frac{T}{V}\sum_Q \Delta_{\mu\nu}(K-Q)\gamma^\mu G^0_{dd}(Q)\pi^-(Q)G_{uu}(Q)\gamma^\nu. \quad (7)$$

Actually, the Dirac structures of $G_{uu}(K)$ and $G_{dd}(K)$ are very simple [6]:

$$G_{uu/dd}(K)=\frac{\tilde k_0 \pm (k-\mu)}{\tilde k_0^2-(E^-_{\boldsymbol{k}})^2}\Lambda_\pm(\boldsymbol{k})\gamma_0+\frac{\tilde k_0 \mp (k+\mu)}{\tilde k_0^2-(E^+_{\boldsymbol{k}})^2}\Lambda_\mp(\boldsymbol{k})\gamma_0, \quad (8)$$

where the dispersions are $E^\pm_{\boldsymbol{k}} = [(k\pm\mu)^2+|\pi^-|^2]^{\frac{1}{2}}$ and the energy projectors are $\Lambda_\pm(\boldsymbol{k}) = (1\pm\gamma_0\gamma\cdot\hat{\boldsymbol{k}})/2$. Writing the pion condensate as $\pi^- = \sum_{s=\pm}\Lambda_s\pi^-_s$, the gap equation becomes

$$\pi_k=\frac{2g^2}{3}\frac{T}{V}\sum_Q \Delta_{\mu\nu}(K-Q)\frac{\pi_q}{\tilde q_0^2-(E^+_{\mathbf{q}})^2}\mathrm{Tr}[\Lambda_-(\boldsymbol{k})\gamma^\mu\Lambda_+(\boldsymbol{q})\gamma^\nu]. \quad (9)$$

Here, because $\mu < 0$, it is enough to consider only $\pi_q \equiv \pi^-_-(Q)$ on the right-hand side. Then, following similar discussions to Ref. [20] and Ref. [21], we can obtain the following gap equation:

$$\pi_k \simeq \bar g^2\int_0^\delta \frac{\pi_q \mathrm{d}(q+\mu)}{Z^{-2}(\tilde E^+_{\boldsymbol{q}})\tilde E^+_{\boldsymbol{q}}}\tanh\left(\frac{\tilde E^+_{\boldsymbol{q}}}{2T}\right)\ln\left(\frac{\tilde b^2\mu^2}{|(\tilde E^+_{\boldsymbol{q}})^2-(\tilde E^+_{\boldsymbol{k}})^2|}\right), \quad (10)$$

where we have defined a constant $\tilde b \equiv 256\pi^4|g|^{-5}$. With the redefinition $z \equiv -(2\bar g^2)^{-1/3}(1-2\bar g x)$ compared to that in Ref. [21], the new forms of Eq. (30) and Eq. (31) in Ref. [21] can be obtained by just taking the combined

transformations: $\bar{g}\to\bar{g}/\sqrt{2}$ and $x\to x\sqrt{2}$. Then we can immediately find from Eq.(33) in Ref. [21] that

$$\Delta = b_\pi |g|^{-5}|\mu_{\rm I}|{\rm e}^{-\frac{\pi}{2\sqrt{2}\bar{g}}},\ b_\pi = 256\pi^4{\rm e}^{-\frac{4+\pi^2}{16}}. \tag{11}$$

Thus, we confirm the expression of the pion condensate as a function of g and $\mu_{\rm I}$ given in Ref. [4, 5] and also find that the coefficient b_π is less suppressed by ${\rm e}^{\frac{4+\pi^2}{16}}\approx 2.38$ compared to that in a color superconductor [21].

3.2 Pure gluodynamics approximation

As shown in Ref. [29], at low temperature, the dynamics of two-flavor color superconductivity is described by a pure $SU(2)$ gluon dynamics at large $\mu_{\rm B}$. Similarly, low-temperature QCD at large $|\mu_{\rm I}|$ is described by $SU(3)$ gluon dynamics in addition to the dynamics of the Goldstone mode [4, 5, 11]. By following the formalism developed in Ref. [11], we can write down the thermodynamic potential as

$$\Omega = \mathcal{U}(\Phi) - \frac{\pi^2}{90}\frac{T^4}{v^3} + \Omega_q, \tag{12}$$

where $v\approx 1/\sqrt{3}$ is the speed of sound and the pure gauge potential is modified from LQCD simulation by changing $T_0 = 270$ MeV to $\tilde{T}_0 = T_0(\tilde{\Lambda}/\Lambda_{\rm QCD})$ [11, 30]:

$$\frac{\mathcal{U}(\Phi)}{T^4} = -\frac{a(T)}{2}\Phi^2 + b(T)\log[1-6\Phi^2+8\Phi^3-3\Phi^4], \tag{13}$$

$$a(T) = a_0 + a_1\left(\frac{\tilde{T}_0}{T}\right) + a_2\left(\frac{\tilde{T}_0}{T}\right)^2,\quad b(T) = b_3\left(\frac{\tilde{T}_0}{T}\right)^3, \tag{14}$$

where the modified confinement scale $\tilde{\Lambda}$ is determined by [11, 29]

$$\alpha(\Delta,\tilde{\Lambda})|_{N_f=0} = \frac{\alpha(\mu_{\rm I},\Lambda)}{\sqrt{\epsilon}} = \frac{\alpha(\mu_{\rm I},\Lambda)}{\sqrt{1+\dfrac{\alpha(\mu_{\rm I},\Lambda)\mu_{\rm I}^2}{72\Delta^2}}}. \tag{15}$$

In order to be more specific, we adopt the four-loop expression for $\alpha(\mu_{\rm I},\Lambda)$ [31]. Inspired by the Polyakov–Nambu–Jona-Lasinio model, the $\mu_{\rm I}$ related quark contribution can be written in the form of free quasi-quarks:

$$\Omega_q = -2\int\frac{{\rm d}^3p}{(2\pi)^3}\sum_{s=\pm}\Big\{N_{\rm c}E^{\rm s}_{\boldsymbol{p}} + 2T\ln\left(1+3\Phi{\rm e}^{-E^{\rm s}_{\boldsymbol{p}}/T}+3\Phi{\rm e}^{-2E^{\rm s}_{\boldsymbol{p}}/T}+{\rm e}^{-3E^{\rm s}_{\boldsymbol{p}}/T}\right)\Big\}, \tag{16}$$

where an ultraviolet regulator is needed and can be implemented by a finite renormalization scale M. Note that the temperature dependence of Δ is neglected, as we are only interested in the low-temperature case $T\ll|\mu_{\rm I}|$.

First, we show the ratios of the isospin density to that in the Stefan-Boltzmann limit $\Delta = 0$, that is, $R_n = n_{\rm I}(\Delta)/n_{\rm I}(0)$ in Fig. 3 for both confined ($\Phi = 0$) and deconfined ($\Phi = 1$) phases. As can be seen, the confinement properties have very little effect on the density at low temperature, and the system can be well described by free quark (antiquark) gas in the whole region as $R_n\approx 1$, especially for $|\mu_{\rm I}| > 5$ GeV, indicating the quarksonic nature. The heat capacity $c_v = T\partial s/\partial T|_{\mu_{\rm I}}$ is explored further as shown in Fig. 4. Although the effective dynamics is pure gluodynamics plus Goldstone mode at low temperature [11], the contribution to c_v is dominated by the Goldstone mode. Just above the deconfinement temperature, the freed gluons start to contribute immediately and further contributions can also come from the quark (antiquark) sea. For higher temperatures, it is dominated by the quark part, when a considerable ratio of the huge quark (antiquark) sea is realised.

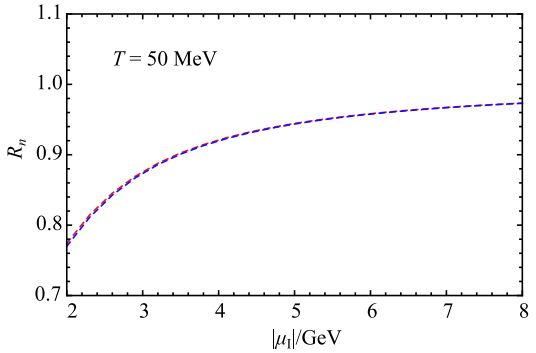

Fig. 3. (color online) The ratios R_n of the isospin density to that in Stefan-Boltzmann limit $\Delta = 0$ as a function of $|\mu_{\rm I}|$ at temperature $T = 50$ MeV. Here, red dotted and blue dashed lines correspond to the confined and deconfined phases, respectively.

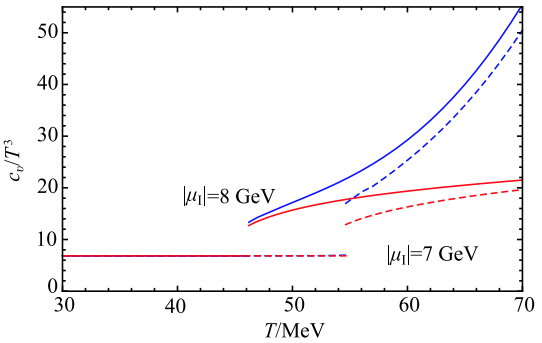

Fig. 4. (color online) The heat capacity c_v as a function of T: the thick blue lines are the total contributions from quarks, gluons, and the Goldstone mode, and the thin red lines are those without contributions from quarks. The solid and dashed lines correspond to $|\mu_{\rm I}| = 8$ GeV and $|\mu_{\rm I}| = 7$ GeV with deconfinement temperatures $T_{\rm d} = 46.19$ MeV and $T_{\rm d} = 54.64$ MeV, respectively. The horizon lines are mainly contributed from the Goldstone mode with $c_v/T^3 = 2\pi^2/15v^3$ independent of $|\mu_{\rm I}|$.

4 Summary

In this Letter, we have argued the existence of a quarksonic matter at large isospin chemical potential $|\mu_{\rm I}|$ in which the quark (antiquark) Fermi seas and confinement coexist. We discussed the physical properties of the quarksonic matter in both large $N_{\rm c}$ and asymptotically free limits. In the large $N_{\rm c}$ limit, we sketched a phase diagram in the $T-|\mu_{\rm I}|$ plane and argued that the quarksonic matter occupies the large $|\mu_{\rm I}|$ (but starting at order $o(N_{\rm c}^0)$) and low temperature region below the deconfinement temperature $T_{\rm d}$, which is independent of $|\mu_{\rm I}|$. For real QCD with $N_{\rm c}=3$, $T_{\rm d}$ decreases with $|\mu_{\rm I}|$ and thus shrinks the quarksonic matter region. In the asymptotically free limit, we first obtain the coefficient b_π which governs the pion condensate gap up to subleading order in the QCD coupling constant. Then, we calculate the isospin density to show that the quark part is indeed a weakly interacting gas at large $|\mu_{\rm I}|$. The heat capacity is mainly contributed from the Goldstone mode at low temperature, and gluons and quarks start to contribute above the deconfinement transition. Compared to quarkyonic matter, the collapse of quarksonic matter is also caused by the deconfinement transition but there are several differences: the latter is also characterized by the existence of pion superfluidity and associated Goldstone mode, which can survive even above the deconfinement transition temperature.

References

1 W. Heisenberg, Z. Phys., **77**: 1 (1932)
2 M. Gell-Mann, Phys. Lett., **8**: 214 (1964)
3 B. A. Li, L. W. Chen, and C. M. Ko, Phys. Rept., **464**: 113 (2008)
4 D. T. Son and M. A. Stephanov, Phys. Rev. Lett., **86**: 592 (2001)
5 D. T. Son and M. A. Stephanov, Phys. Atom. Nucl., **64**: 834 (2001); Yad. Fiz., **64**: 899 (2001)
6 L. He, M. Jin, and P. Zhuang, Phys. Rev. D, **71**: 116001 (2005)
7 L. He, M. Jin, and P. Zhuang, Phys. Rev. D, **74**: 036005 (2006)
8 G. Sun, L. He, and P. Zhuang, Phys. Rev. D, **75**: 096004 (2007)
9 C. f. Mu, L. y. He, and Y. x. Liu, Phys. Rev. D, **82**: 056006 (2010)
10 L. He, Phys. Rev. D, **82**: 096003 (2010)
11 T. D. Cohen and S. Sen, Nucl. Phys. A, **942**: 39 (2015)
12 T. Brauner and X. G. Huang, arXiv:1610.00426 [hep-ph]
13 J. B. Kogut and D. K. Sinclair, Phys. Rev. D, **66**: 034505 (2002)
14 J. B. Kogut and D. K. Sinclair, Phys. Rev. D, **70**: 094501 (2004)
15 G. S. Bali, G. Endrodi, R. V. Gavai, and N. Mathur, arXiv: 1610.00233 [hep-lat]
16 L. McLerran and R. D. Pisarski, Nucl. Phys. A, **796**: 83 (2007)
17 V. V. Braguta, E.-M. Ilgenfritz, A. Y. Kotov, A. V. Molochkov, and A. A. Nikolaev, arXiv:1605.04090 [hep-lat]
18 T. Brauner, K. Fukushima and Y. Hidaka, Phys. Rev. D, **80**: 074035 (2009); Phys. Rev. D, **81**: 119904 (2010)
19 M. Hanada and N. Yamamoto, PoS LATTICE, **2011**: 221 (2011)
20 R. D. Pisarski and D. H. Rischke, Phys. Rev. D, **61**: 074017 (2000)
21 Q. Wang and D. H. Rischke, Phys. Rev. D, **65**: 054005 (2002)
22 G. 't Hooft, Nucl. Phys. B, **72**: 461 (1974)
23 P. Kovtun, M. Unsal, and L. G. Yaffe, JHEP, **0706**: 019 (2007)
24 Y. Hidaka and N. Yamamoto, Phys. Rev. Lett., **108**: 121601 (2012).
25 W. E. Brown, J. T. Liu, and H. c. Ren, Phys. Rev. D, **61**: 114012 (2000)
26 W. E. Brown, J. T. Liu, and H. c. Ren, Phys. Rev. D, **62**: 054013 (2000) .
27 W. E. Brown, J. T. Liu, and H. c. Ren, Phys. Rev. D, **62**: 054016 (2000)
28 C. Manuel, Phys. Rev. D, **62**: 076009 (2000)
29 D. H. Rischke, D. T. Son, and M. A. Stephanov, Phys. Rev. Lett., **87**: 062001 (2001)
30 S. Roessner, C. Ratti, and W. Weise, Phys. Rev. D, **75**: 034007 (2007)
31 K.A. Olive et al (Particle Data Group), Chin. Phys. C, **38**: 090001 (2014)